

# Driving as a Diagnostic Tool: Scenario-based Cognitive Assessment in Older Drivers from Driving Video

Md Zahid Hasan<sup>a</sup>, Guillermo Basulto-Elias<sup>b</sup>, Jun Ha Chang<sup>c</sup>, Sahuna Hallmark<sup>b</sup>, Matthew Rizzo<sup>c</sup>, Anuj Sharma<sup>b</sup>, Soumik Sarkar<sup>d</sup>

<sup>a</sup>*Department of Electrical & Computer Engineering, Iowa State University, Ames, IA, 50011, USA*

<sup>b</sup>*Institute for Transportation, Iowa State University, Ames, IA, USA*

<sup>c</sup>*Mind and Brain Health Lab, University of Nebraska Medical Center, Omaha, NE, USA*

<sup>d</sup>*Department of Mechanical Engineering, Iowa State University, Ames, IA, USA*

---

## Abstract

We introduce scenario-based cognitive status identification in older drivers from naturalistic driving videos, leveraging large vision models. In recent times, cognitive decline including Dementia and Mild Cognitive Impairment (MCI), is often underdiagnosed due to the time-consuming and costly nature of current diagnostic methods. By analyzing real-world driving behavior captured through in-vehicle sensors, this study aims to extract “digital fingerprints” that correlate with functional decline and clinical features of dementia. Moreover, modern large vision models can draw meaningful insights from everyday driving patterns across different roadway scenarios to early detect cognitive decline. We propose a framework that uses large vision models and naturalistic driving videos to analyze driver behavior, identify cognitive status and predict disease progression. We leverage the strong relationship between real-world driving behavior as an observation of the current cognitive status of the drivers where the vehicle can be utilized as a “diagnostic tool”. Our method identifies early warning signs of functional impairment, contributing to proactive intervention strategies. This work enhances early detection and supports the development of scalable, non-invasive monitoring systems to mitigate the growing societal and economic burden of cognitive decline in the aging population.

### *Keywords:*

Naturalistic driving, Vision model, Cognitive decline, Driving scenario

---

## 1. Introduction

Cognitive decline in the aging population is a critical health concern that manifests across a spectrum of stages. The pre-dementia stage, commonly referred to as mild cognitive impairment (MCI), is characterized by measurable cognitive impairment with minimal or no functional changes in daily living [1, 2]. Individuals at this stage (often in their 70s) may exhibit early signs of cognitive decline without severe disruptions to independence. As the condition progresses to dementia, more severe cognitive and functional impairments emerge, ultimately diminishing the ability to live independently [3]. While MCI is not exclusive to dementia, it often serves as an early indicator of the disease and highlights the need for early detection and intervention [4].

The timely identification of MCI provides an opportunity to slow disease progression, improve quality of life, and reduce the societal burden associated with advanced stages of dementia. Traditional methods for diagnosing cognitive decline are often time-consuming, costly, and reliant on clinical visits or complex neuroimaging techniques, which may not be practical for widespread use [2, 5, 6]. To address this, our research explores an innovative approach using real-world driving behavior as a passive diagnostic tool [7, 8]. This study focuses on individuals exhibiting MCI due to mild dementia, as determined by clinical characteristics [9].

Prior research on cognitive decline has explored a variety of methods to detect early changes in individuals at risk of dementia. Neuroimaging techniques, such as magnetic resonance imaging (MRI) [10, 11] and positron emission tomography (PET) [12, 13] have been widely used to identify structural and functional brain changes associated with dementia. These methods are often paired with biomarkers, such as amyloid-beta and tau proteins [14], blood-based biomarkers [15] to improve diagnostic accuracy. However, the high cost and limited accessibility of these techniques hinder their widespread application [16]. Wearable sensor technologies [17, 18] have also gained traction in recent years. Studies have demonstrated the utility of devices that monitor gait patterns, heart rate variability, and sleep quality to assess functional and cognitive impairments. Machine learning models [19, 20, 21] applied to sensor data have shown promise in predicting the progression of cognitive decline. However, these approaches often require participant compliance and are limited to specific contexts, such as controlled environments or clinical trials [22]. Some studies [23, 24, 25] demonstrated that everyday driving behavior, such as reduced driving distances, fewer unique destinations,

and smaller driving spaces, is associated with symptomatic MCI. However, limited research has investigated the impact of preclinical MCI on driving behavior [26, 27], highlighting a critical gap in understanding early-stage cognitive decline. Recently, driving research has shifted towards naturalistic assessments using sensor devices installed in participants’ personal vehicles, enabling the collection of real-world driving behavior data [7, 26].

While neuropsychological testing provides a comprehensive assessment of cognitive abilities, it often requires in-person clinical visits, participant compliance, and substantial time and resources — all of which may be challenging for individuals in the early stages of MCI [28]. In this context, our approach capitalizes on passive monitoring of real-world driving behavior, which offers a non-invasive, cost-effective, and scalable solution. Analyzing naturalistic driving data offers a promising alternative to capture subtle behavioral cues of cognitive decline in real-world settings [29, 30]. Studies show that behavioral patterns in everyday driving can be an alternative and effective approach to detect early-stage MCI, complementing traditional cognitive testing and potentially enabling earlier intervention [29, 31, 26]. By combining driving video data with advanced computer vision techniques, we aim to discover the relationship between driving behavior and cognitive assessment, providing a digital “diagnostic tool” for early detection of cognitive decline. We propose a scenario-based framework that identifies discriminative behavioral cues and shows how scenario-specific analysis can reveal early cognitive decline more effectively than aggregate driving metrics.

## 2. Methodology

### 2.1. RWRAD Dataset

The dataset was collected in collaboration with the University of Nebraska Medical Center (UNMC) and includes comprehensive neuropsychological assessments, clinical tests and naturalistic driving data aimed at investigating cognitive impairment and its progression among older adults.

#### 2.1.1. Participants

These data were derived from a cohort of community-dwelling older adults (aged 65 - 90 years) enrolled in longitudinal studies on dementia and driving behavior, conducted at the UNMC Mind and Brain Health Labs between March 2021 and January 2024. Recruitment procedures followed prior work [32, 29], involving community outreach efforts (e.g., flyers, social media,

local news, discussions at senior organizations) and pre-screening to ensure eligibility based on defined inclusion criteria (see Appendix A). All participants lived independently in Nebraska or neighboring states (e.g., Iowa), held a valid driver’s license, were proficient in English and provided informed consent. Exclusion criteria were applied to minimize potential confounding effects from underlying health conditions and are detailed in Appendix A. The study protocol was approved by the UNMC Institutional Review Board (IRB 0522-20-FB) and all participants provided written informed consent prior to participation. A summary overview of the participants is shown in Table 1.

### *2.1.2. Data collection*

Data collection includes recording driving video, sensor signals, actigraphy, sleep log, driving behavior and in-lab cognitive assessment conducted at UNMC. Over a 2-year period, driving data were collected in 3-month intervals using custom-installed “Black Box” systems in each participant’s personal vehicle. The system continuously recorded driving behavior throughout each trip over a 12-week period. It captured synchronized video (front roadway and cabin), vehicle sensor data (GPS, accelerometer, gyroscope), and on-board diagnostics data (speed, rpm, engine throttle). All data were recorded at a 1Hz sampling rate from engine start to stop (ignition cycle). Each ignition cycle indicates a distinct “drive” for the corresponding driver, excluding trips with zero mileage or speed < 5mph (e.g., parking lot or driveway maneuvers) or if participants reported periods of non-driving (e.g., vacations, illness).

### *2.1.3. Cognitive Status*

Cognitive status was determined using the 2018 NIA-AA research criteria [9]. To assess cognitive status, participants completed a series of tests across five domains – memory, language, visuospatial abilities, executive function and attention (see Appendix B). Specialist clinicians in dementia and Alzheimer’s reviewed the neuropsychological evaluations for cognition and daily functioning from the National Alzheimer’s Coordinating Center (NACC) Unified Data Set (UDS) version 3 [33]. They reached a consensus on cognitive staging based on participants performance across the five cognitive domains. Raw test scores were converted into standardized  $Z$ -scores, adjusted for age, sex, and education. These  $Z$ -scores were then used to define cognitive impairment. As cognitive impairment progresses, it often becomes

Table 1: Summary characteristics of the participants in RWRAD dataset

Variable	Range or Counts	Average	Std. Dev.
Age (years)	Range: 65 - 90	75.4	6.0
Sex	Female: 75 Male: 61	-	-
Race	White: 125 Black: 9 American Indian: 1 Other: 1	-	-
Income	\$0 - \$100,000 Not indicated: 86	\$43,026.43	\$27,855.35
Employment	Employed full/part time: 19 Retired: 107 Volunteering: 9 Keeping house: 1	-	-
Driving Experience (years)	Range: 45 - 78	58.7	6.6
Weekly Driving (miles)	Range: 5 - 300	85.9	75.2
COGSTAT Score	Range: 300 - 800	643.22	106.52
MoCA Score	Range: 15 - 30	24.3	3.4

a multi-domain process, ultimately impacting functional abilities and transitioning to the dementia stage. The in-lab data collection focused on assessing functional abilities and activities through driving behavior in various roadway scenarios. Cognitive performance was evaluated using two composite cognitive scores. First, the COGSTAT score was utilized as a measure of cognitive function [34]. It was derived from 14 neuropsychological tests evenly distributed across those five cognitive domains. For each test, an age-adjusted  $Z$ -score was calculated and transformed into a  $T$ -score (mean = 50, SD = 10) using the formula  $T = 10(Z \times 10 + 50)$ . The composite scores required complete data without missing tests to ensure validity. Second, the Montreal Cognitive Assessment (MoCA) score was used as a clinical screening tool designed to detect clinically significant cognitive change and age-related cognitive decline [35]. Both the MoCA and the full neuropsychological bat-

tery were administered to all participants. To address challenges associated with compliance and self-reporting accuracy in cognitively impaired participants, a study partner was recruited for each participant. After two weeks, participants returned to the study site with their partner for evaluations of cognitive status and daily functioning.

Participants were classified based on the presence of both cognitive and functional decline. Those without any impairment in cognition or daily functioning were labeled as cognitively unimpaired (CU) or “Normal-aging”. Individuals who demonstrated cognitive decline but maintained functional independence were classified as having mild cognitive impairment (MCI). When cognitive decline was accompanied by functional impairment, participants were considered to have dementia. Given the small number of dementia cases ( $N = 9$ ), participants with MCI and dementia were combined into a single category termed Mild Dementia (MD) or “MD-aging”, similar to stage 4 in [9]. Clinical evaluation of MCI is primarily a rule-out process aimed at determining whether the primary impairment is due to another type of dementia. However, the majority of people with Alzheimer’s ( $\sim 60\%$ ) also have other types of dementia [36]. While this study does not exclude individuals with co-morbid dementias, clinical assessments were designed to capture these data.

## 2.2. Video Data Processing

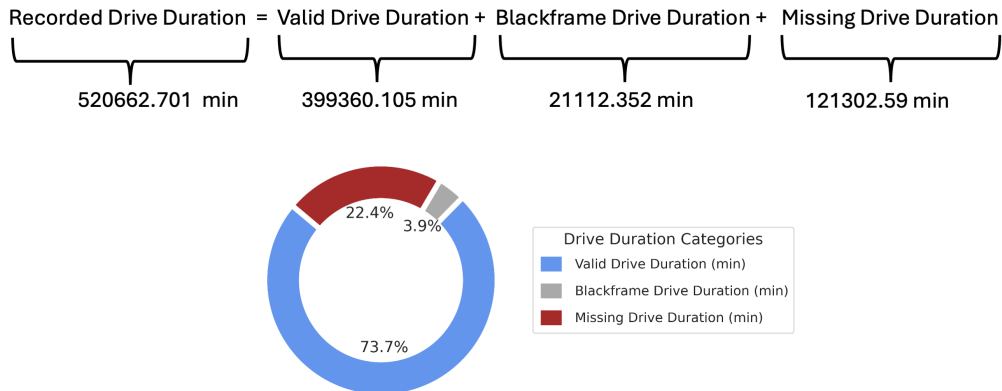


Figure 1: Breakdown of the driving data in the RWRAD dataset

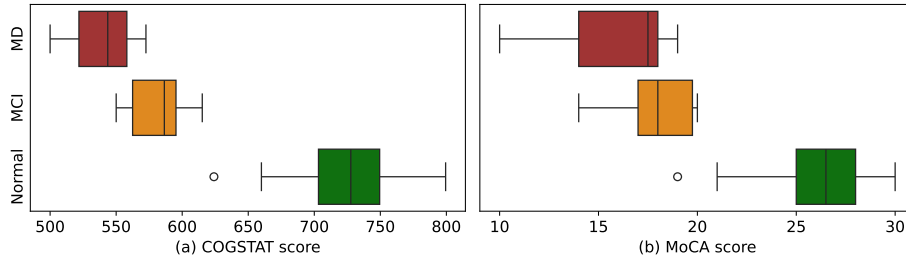


Figure 2: Cognitive score (a) COGSTAT, (b) MoCA distribution across subjects ( $N = 69$ ). We combined the MD and MCI subjects into a unified class “MD-aging” and performed two-class classification with the “Normal-aging”.

Quality driving video is essential for reliable video-based modeling since missing or corrupted data can hurt the validity of findings. Ensuring rigorous processing of the collected video clips was therefore a crucial step before conducting our analysis. While processing the collected driving video data, we encountered some missing and corrupted video clips that required filtering and formatting. Figure 1 presents the breakdown of the processed driving data for the RWRAD dataset. The in-vehicle **Blackbox** system recorded a total of 520,662.7 minutes of driving data, segmented into valid drive duration (73.7%), Blackframe drive duration (3.9%) and Missing drive duration (22.4%). For the video-based analysis, only valid driving data was retained. Drives with missing or corrupted data and Black-frame data were excluded to ensure input data quality and consistency for driver behavior modeling.

Subjects with their corresponding driving videos were filtered out for only those drives that occurred on the **Omaha most transited route**, a predefined set of road segments derived from the RWRAD dataset (see Figure 3). This criterion was applied to ensure adequate video data coverage for each participant and to make sure we have diverse driving scenario exposure in the video samples. In addition, the common driving route ensures that individual drivers commute on a shared set of road segments, reducing variability due to route differences. This allows the model to focus on relevant driving patterns rather than route features. For our analysis, a total of  $N = 69$  subjects were filtered out, after excluding the subjects without cognitive status labels and drivers outside the Omaha region. Figure 2 shows the distribution of the cognitive scores across three aging groups— MD, MCI, and Normal. Among 69 subjects, 35 drivers (26 MCI and 9 MD combined) were categorized as “MD-aging”, while 34 were classified as “Normal-aging”. This balanced dis-

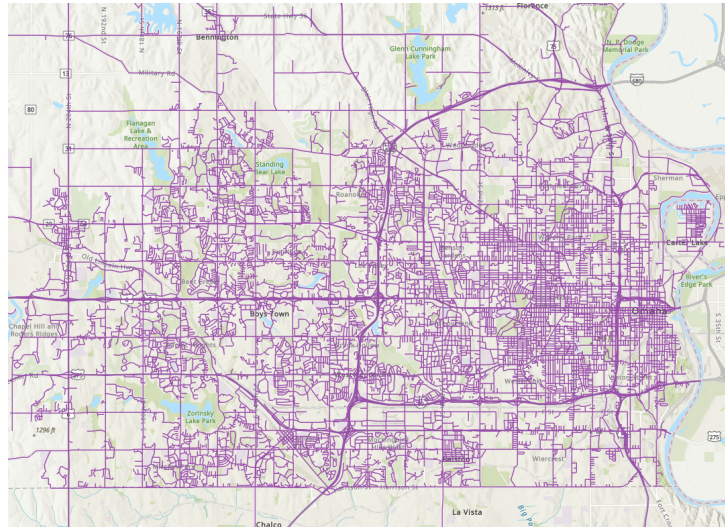


Figure 3: GIS map of the Omaha most transited route database (Omaha, NE)

tribution enabled a robust comparison between normal and MD-aging groups in terms of cognitive test scores and driving behavior. The MD-aging subjects consistently show the lowest cognitive scores, while normal-aging individuals cluster at the higher end. MCI subjects span the intermediate range, overlapping with both groups. It also highlights the transitional nature of cognitive decline and the inherent classification challenge.

To ensure consistency and relevance in our analysis, we focused on short driving segments. We selected roadway segments where the drive distance can be  $\leq 0.31$  mile or  $\leq 500$  meters and defined it as a “route segment” (discussed in 3.1). These segments provide concentrated snapshots of driver behavior under controlled road conditions. This approach minimizes variability due to changes in driving context or prolonged periods of noisy observation. Additionally, the time of day and traffic conditions (peak vs. off-peak hours) were considered to account for environmental stressors that could uniquely challenge drivers with mild dementia. Next, the scenario-specific video sampling method is described in section 2.3.

### 2.3. Scenario-specific Video Sampling

The overall pipeline for scenario-specific video sampling is illustrated in Figure 4. Let  $\mathcal{D} = D_1, D_2, \dots, D_d$  be the set of subjects that were filtered out in section 2.2. Each subject  $D_i$  performed a set of drives  $\{dr_1, dr_2, \dots, dr_n\}$

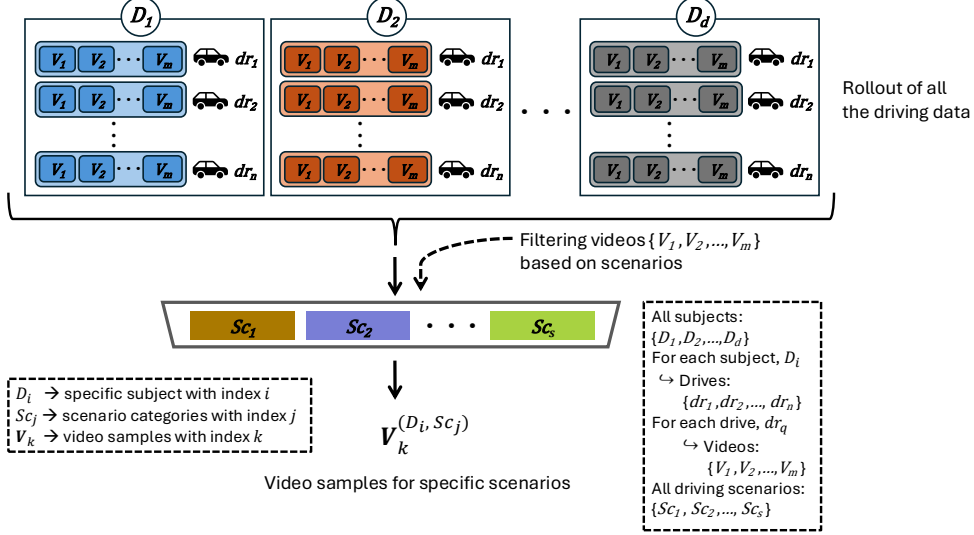


Figure 4: Scenario-specific video sampling. The top row represents the rollout of all valid drives and driving videos across subjects in the **Omaha most transited route**. From each subject  $D_i$ , valid drives  $\{dr_1, dr_2, \dots, dr_n\}$  and their associated video samples  $\{V_1, V_2, \dots, V_m\}$  were mapped into scenario-specific subsets. These video samples were aggregated and used as input to the large vision model for driving pattern analysis.

where  $n$  is the maximum number of drives per subject. Each drive was further segmented into short video clips  $\{V_1, V_2, \dots, V_m\}$ , where  $m$  is the maximum number of video clips per drive. These video clips were recorded under different driving scenarios,  $\mathcal{S} = Sc_1, Sc_2, \dots, Sc_s$ . From these video clips, a subset of scenario-specific video samples  $V_k^{(D_i, Sc_j)}$  was filtered for each subject-scenario pair  $(D_i, Sc_j)$  where  $k$  is the index of the sampled video clip,  $i$  is the index of the subject and  $j$  is the index of the scenario. This resulted in a quality dataset of labeled video samples that were used as inputs to the large vision model in the next stage. This sampling strategy ensures sufficient data representation across both aging groups (Normal vs. MD) and allows the proposed method to be validated on balanced and identical driving scenarios. Additionally, the hierarchical video sampling steps across subjects, drives, and scenarios ensure a structured and scalable representation across varying cognitive profiles and driving contexts.

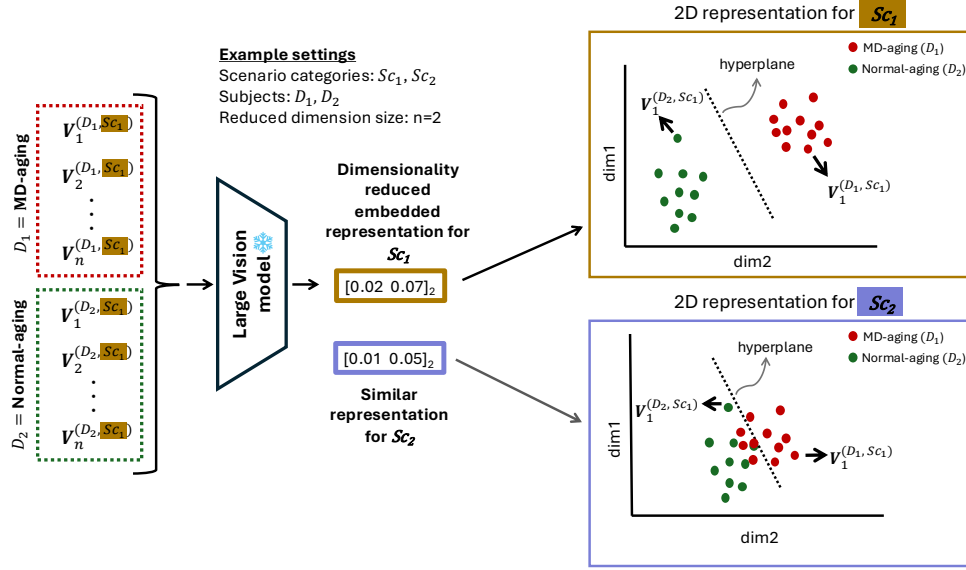


Figure 5: Overview of the large vision model-based framework. Given, the input video segments  $\mathcal{V} = \{V_k^{(D_i, Sc_j)}\}$  where  $i = 1, \dots, d$ ;  $j = 1, \dots, k$ ;  $k = 1, \dots, n$  from different scenarios  $Sc_j \in \mathcal{S}$ , a vision model  $F_\theta$  mapped each  $V_i$  to a vector space  $Z_i = F_\theta(V_i) \in \mathbb{R}^m$ . The vector space was analyzed to assess inter-group separation using a distance metric. Scenario  $Sc_1$  showed significant class-wise separation than  $Sc_2$ , i.e.,  $\text{Dist}_{Sc_1} > \text{Dist}_{Sc_2}$ , indicating higher discriminative potential for distinguishing the cognitive groups.

#### 2.4. Large Vision Model-based Framework

The video samples derived in section 2.3 were fed into a pre-trained large Vision Transformer model [37] to generate vectorized representations of the video data. The objective of this framework is to encode driving videos into discriminative vector representations for downstream classification of cognitive aging groups. These representations capture prominent visual features that contrast the driving behavior of the two cognitive groups and distinguish them based on the vector's distance in feature space (illustrated in Figure 5). The entire framework includes four steps as follows:

##### Step 1: Video-to-vector generation

Each video sample  $V_k^{(D_i, Sc_j)}$  is passed through a pre-trained large vision model  $F_\theta$  to obtain a fixed-size vector space:

$$Z_k = F_\theta(V_k^{(D_i, Sc_j)}), \quad Z_k \in \mathbb{R}^m$$

where  $Z_k$  denotes the vector representation of each video sample  $V_k^{(D_i, S_{c_j})}$  in an  $m$ -dimensional latent space.

### Step 2: Dimensionality Reduction

To interpret the structure of the vector space and the separability of the aging groups in each scenario setting, we apply PCA [38], a dimensionality reduction function  $g : \mathbb{R}^m \rightarrow \mathbb{R}^n$  to obtain:

$$\tilde{Z}_k = g(Z_k), \quad \tilde{Z}_i \in \mathbb{R}^n, \text{ where } n \in \{50, 100, 200\}, n \ll m$$

This step was performed in a way to preserve the majority of the information embedded in the high-dimensional video representation while mapping it into a low-dimensional vector space. It allows us to observe how the visual features related to the driving behavior in different scenarios for the two aging groups are clustered in a low-dimensional feature space.

### Step 3: Discriminative Scenario Selection

To evaluate the relevance of a scenario  $S_{c_j} \in \mathcal{S}$  for distinguishing the two aging groups, we computed a class-wise Euclidean distance in the reduced feature space. In Figure 5, an example of a dimension-reduced representation ( $n = 2$ ) with the group separability in feature space is illustrated. The Euclidean distance between the class centroids was obtained as follows:

$$\boldsymbol{\mu}_{\text{normal}}^{(S_{c_j})} = \frac{1}{|\tilde{Z}_{\text{normal}}^{(S_{c_j})}|} \sum_{\mathbf{z} \in \tilde{Z}_{\text{normal}}^{(S_{c_j})}} \mathbf{z}, \quad \boldsymbol{\mu}_{\text{MD}}^{(S_{c_j})} = \frac{1}{|\tilde{Z}_{\text{MD}}^{(S_{c_j})}|} \sum_{\mathbf{z} \in \tilde{Z}_{\text{MD}}^{(S_{c_j})}} \mathbf{z}$$

Here,  $\tilde{Z}_{\text{normal}}^{(S_{c_j})}$  and  $\tilde{Z}_{\text{MD}}^{(S_{c_j})}$  denote the sets of low-dimensional vectors under scenario  $S_{c_j}$  for the Normal and MD-aging groups respectively. Each centroid  $\boldsymbol{\mu}_{\text{normal}}^{(S_{c_j})}, \boldsymbol{\mu}_{\text{MD}}^{(S_{c_j})} \in \mathbb{R}^n$  represents the average position of the corresponding group in the feature space for the same scenario. The Euclidean distance between the two centroids was then obtained by:

$$\text{Dist}(S_{c_j}) = \left\| \boldsymbol{\mu}_{\text{normal}}^{(S_{c_j})} - \boldsymbol{\mu}_{\text{MD}}^{(S_{c_j})} \right\|_2$$

Then,  $\text{Dist}(S_{c_j})$  is used to determine the most discriminative scenario as:

$$S_{c_{\max}} = \arg \max_{S_{c_j} \in \mathcal{S}} \text{Dist}(S_{c_j})$$

where  $S_{c_{\max}}$  denotes the most discriminative scenario that maximizes the inter-group distance between the Normal and MD-aging groups centroids in the feature space.

#### Step 4: Validation of Scenario Selection

To validate the scenario selection, two identical Random Forest (RF) [39] classifiers were trained and evaluated on the *most* and *least* discriminative scenarios obtained in Step 3. In addition to the most discriminative scenario, we calculated the least discriminative scenario as:

$$Sc_{\min} = \arg \min_{Sc_j \in \mathcal{S}} \text{Dist}(Sc_j)$$

Let  $\tilde{\mathcal{Z}}^{(Sc)} = \{\tilde{Z}_k^{(Sc)}\}$  denotes the reduced dimensional vectors (from Step 2) and  $\mathcal{Y}^{(Sc)} = \{Y_k^{(Sc)}\}$  their corresponding labels for scenario  $Sc \in \{Sc_{\max}, Sc_{\min}\}$ . We trained two RF classifiers with identical hyperparameters on the reduced feature space for both scenarios  $\{Sc_{\max}, Sc_{\min}\}$ :

$$\hat{Y}_k^{(Sc)} = \tilde{H}^{(Sc)}\left(\tilde{Z}_k^{(Sc)}\right), \quad \tilde{H}^{(Sc)} : \mathbb{R}^n \rightarrow \mathcal{Y},$$

A balanced train-test split and a  $K$ -fold cross-validation step were used to balance the two aging groups data for training the RF classifiers. Then the trained RF models performance was assessed on classification accuracy(**a**), precision(**P**), recall(**R**) and F1-score(**F1**) computed on the test data for each scenario. Finally, we compared

$$\{\mathbf{a}, \mathbf{P}, \mathbf{R}, \mathbf{F1}\}_{Sc_{\max}} \quad \text{vs.} \quad \{\mathbf{a}, \mathbf{P}, \mathbf{R}, \mathbf{F1}\}_{Sc_{\min}}$$

and reported the performance difference as a validation criterion. A consistent performance gain of  $\tilde{H}^{(Sc_{\max})}$  over  $\tilde{H}^{(Sc_{\min})}$  validates the proposed scenario-based approach by demonstrating that scenarios with larger inter-centroid separation yield stronger discriminability between the two cognitive aging groups. The entire framework is shown in Algorithm 1. Moreover, we further evaluated the validity of the framework under different data sampling strategies. Multiple sampling strategies (random and driver-level separation) were employed to assess whether the observed RF classifier performance generalizes across subjects and settings. We reported the average performance **a**, **P**, **R**, and **F1** under two complementary sampling strategies:

---

**Algorithm 1** Scenario-Based Video Analysis
 

---

```

1: Input: Video samples  $\mathcal{V} = \{V_k^{(D_i, Sc_j)}\}$ , subjects  $\mathcal{D}$ , scenarios  $\mathcal{S}$ , vision
   model  $F_\theta$ , PCA  $g : \mathbb{R}^m \rightarrow \mathbb{R}^n$ , sampling method  $\mathbf{S} \in \{\text{Random, DLS}\}$ 
2: Output: Scenario ranking  $\{\text{Dist}(Sc_j)\}_{Sc_j \in \mathcal{S}}$ , trained RFs  $\{\mathbf{a}, \mathbf{P}, \mathbf{R}, \mathbf{F1}\}$ 
3: for each scenario  $Sc_j \in \mathcal{S}$  do
4:    $\mathcal{E}_{Sc_j} \leftarrow \emptyset$ 
5:   for each subject  $D_i \in \mathcal{D}$  do
6:     for each video  $V_k^{(D_i, Sc_j)}$  do
7:        $Z_k \leftarrow F_\theta(V_k^{(D_i, Sc_j)})$  ▷ Step 1
8:        $\mathcal{E}_{Sc_j} \leftarrow \mathcal{E}_{Sc_j} \cup \{Z_k\}$ 
9:     end for
10:  end for
11:   $\tilde{\mathcal{E}}_{Sc_j} \leftarrow g(\mathcal{E}_{Sc_j})$  ▷ Step 2
12:  Divide  $\tilde{\mathcal{E}}_{Sc_j}$  into class-wise sets  $\tilde{Z}_{\text{normal}}^{(Sc_j)}, \tilde{Z}_{\text{MD}}^{(Sc_j)}$ 
13:   $\boldsymbol{\mu}_{\text{normal}}^{(Sc_j)} \leftarrow \frac{1}{|\tilde{Z}_{\text{normal}}^{(Sc_j)}|} \sum_{\mathbf{z} \in \tilde{Z}_{\text{normal}}^{(Sc_j)}} \mathbf{z}$ ,  $\boldsymbol{\mu}_{\text{MD}}^{(Sc_j)} \leftarrow \frac{1}{|\tilde{Z}_{\text{MD}}^{(Sc_j)}|} \sum_{\mathbf{z} \in \tilde{Z}_{\text{MD}}^{(Sc_j)}} \mathbf{z}$ 
14:   $\text{Dist}(Sc_j) \leftarrow \left\| \boldsymbol{\mu}_{\text{normal}}^{(Sc_j)} - \boldsymbol{\mu}_{\text{MD}}^{(Sc_j)} \right\|_2$  ▷ Step 3
15: end for
16:  $Sc_{\max} \leftarrow \arg \max_{Sc_j \in \mathcal{S}} \text{Dist}(Sc_j)$  ▷ most discriminative scenario
17:  $Sc_{\min} \leftarrow \arg \min_{Sc_j \in \mathcal{S}} \text{Dist}(Sc_j)$  ▷ least discriminative scenario
18: for each  $Sc \in \{Sc_{\max}, Sc_{\min}\}$  do
19:    $(\mathbf{X}^{(Sc)}, \mathbf{y}^{(Sc)}) \leftarrow (\tilde{\mathcal{E}}_{Sc}, \text{labels})$ 
20:   if  $\mathbf{S} = \text{Random}$  then
21:     Stratified train/val/test split on samples (balanced)
22:   else if  $\mathbf{S} = \text{DLS}$  then
23:     Leave- $k$ -drivers-out: hold out  $k$  drivers as test set; repeat  $r$  runs
     with different held-out drivers
24:   end if
25:   Train RF  $\tilde{H}^{(Sc)} : \mathbb{R}^n \rightarrow \mathcal{Y}$  on train split ▷ Step 4
26:   Evaluate on held-out data to obtain  $\{\mathbf{a}, \mathbf{P}, \mathbf{R}, \mathbf{F1}\}_{Sc}$ ; average over
     runs if DLS
27: end for
28: return  $\{\text{Dist}(Sc_j)\}_{Sc_j \in \mathcal{S}}, \{\mathbf{a}, \mathbf{P}, \mathbf{R}, \mathbf{F1}\}_{Sc_{\max}}, \{\mathbf{a}, \mathbf{P}, \mathbf{R}, \mathbf{F1}\}_{Sc_{\min}}$ 

```

---

- **Random Sampling:** A total of  $n$  video samples are randomly selected from the full dataset for training and testing, without enforcing subject-

or scenario-level separation. This strategy evaluates the model’s performance under unconstrained sampling conditions.

- **Driver-level Separation (DLS):** To evaluate the generalizability of the proposed framework across different individuals, we employed a leave- $k$ -drivers-out cross-validation strategy [40], where  $k$  drivers were excluded from the training set and reserved exclusively for testing. This procedure was repeated over  $r$  independent runs, each with a different subset of left-out drivers. Finally, the results across these runs were averaged to get the final performance metrics ( $\mathbf{a}, \mathbf{P}, \mathbf{R}, \mathbf{F1}$ ). It ensures robustness and mitigates variance due to subject-specific biases.

This sampling strategy evaluates both intra-subject consistency (random) and inter-subject generalization (DLS) in the proposed modeling approach.

### 3. Experimental Setup

#### 3.1. Scenario-based Roadway Selection

To investigate the connection between driving behavior and cognitive status, we tested and selected two distinct scenarios from the **Omaha most transited route** where older drivers exhibited the most discriminative driving patterns. These patterns can serve as interpretable behavioral cues for identifying cognitive decline. The selected driving scenarios are:

- **Freeway-interchange:** merging or diverging behavior in ramp entries or exit segments. e.g., JFK N to I-80 E Ramp, I-480 W to Dodge W Ramp.
- **Interstate:** high-speed, lane-keeping scenarios on long uninterrupted roads. e.g., Omaha I-80 W, I-80 E.

From different federal functional categories (e.g., Local, Major collector, Minor collector, etc.), we selected the most contrastive scenario combination and performed scenario-specific video sampling as section 2.3. Figure 6 shows the GIS map highlighting the two driving scenarios for our analysis. We considered a single drive having  $\leq 0.31$  miles or  $\leq 500$  meters in length as a route segment. **Omaha most transited route** database consists of 24,106 route segments. In total, we filtered out 964 unique route segments, consisting of 632 freeway-interchange segments (highlighted in green on Figure 6(b))

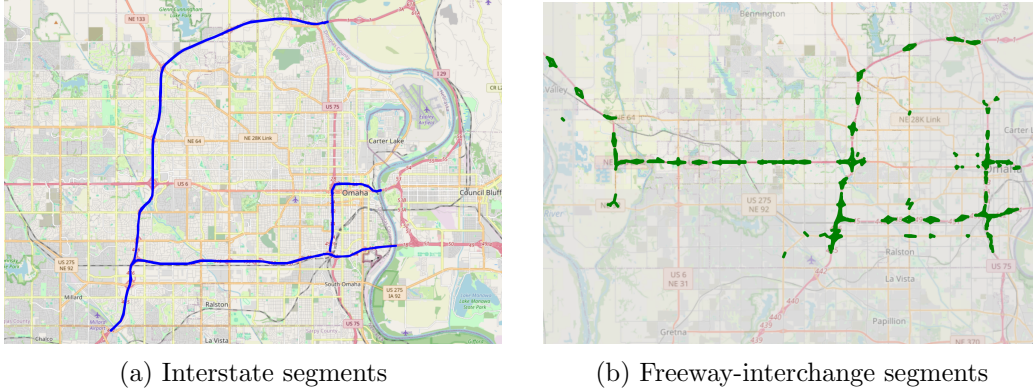


Figure 6: GIS map - (a) Interstate and (b) Freeway-interchange scenarios. The relevant route segments were filtered out from the Omaha most transited route database shown in Figure 3.

and 332 interstate segments (highlighted in blue on Figure 6(a)). Table 2 summarizes the key statistics – a balance of the selected data and driving exposure of the cognitive groups. Additionally, we selected the route segments that cover at least a minimum number of drives for both cognitive groups. To interpret the driving exposure data distribution in Table 2, we defined several key variables below:

- $N_u$ : Number of unique trips by the Normal-aging subjects
- $C_u$ : Number of unique trips by the subjects with MCI
- $M_u$ : Number of unique trips by the subjects with MD
- $T_u$ : Total unique trips across all subject groups  
 $T_u = N_u + C_u + M_u$   
 It does not include repeated trips which means multiple driving sessions recorded on the same route segment by the same individuals
- $\bar{T}_u$ : Total number of trips including repeated ones (non-unique).  
 It includes repeated trips which means multiple driving sessions recorded on the same drive segment by the same individual.
- $T_{rep}$ : The average number of times each unique trip was repeated per subject on a route segment, defined as  $T_{rep} = \frac{\bar{T}_u}{T_u}$ . It gives an approximation of how often participants repeated drives on a certain route

segment. For example, each unique interstate trip was repeated 4.41 times, compared to 3.55 times for freeway interchange trips. Therefore, participants tended to repeat trips on interstate route segments more frequently than on the freeway interchanges.

Table 2: Driving exposure in the route segments for two scenarios

Scenario categories	Normal trips( $N_u$ )	MCI trips( $C_u$ )	MD trips( $M_u$ )	Unique trips( $T_u$ )	Recurring trips( $\bar{T}_u$ )	Recurring trip factor( $T_{rep}$ )
Fwy-int.	8136	10134	919	19189	68048	3.55
Interstate	7123	7894	780	15797	69620	4.41

$N_u$ : unique trips by Normal group;  $C_u$ : unique trips by MCI group;  $M_u$ : unique trips by MD group;  $T_u$ : total unique trips;  $\bar{T}_u$ : total non-unique trips; Fwy-int.: Freeway interchange.

We leveraged “unique drives” vs. “repeated drives” per subject across all the route segments to indicate statistical reliability and diversity in driving exposure by the two cognitive groups. The recurring trips per subject suggest that each participant had substantial driving trips with the selected roadway scenario, offering a significant amount of video data for our analysis.

Figure 7 shows a boxplot distribution of speed limits and the trip distance for both scenarios. As we observed, the freeway-interchange segments tend to have lower speed limits and shorter distances, which work as a transitional driving scenario, involving challenging driving maneuvers and fast decision-making. In contrast, the interstate segments exhibit higher speed limits and longer travel distances, which indicate an uninterrupted highway driving scenario with relaxed driving behavior.

- Median speed limits:  
Fwy-interchange scenario,  $S_{fwy} = 37.5$  mph  
Interstate scenario,  $S_{int} = 60$  mph
- Median distances:  
Fwy-interchange scenario,  $D_{fwy} = 0.12$  miles  
Interstate scenario,  $D_{int} = 0.20$  miles

These characteristics offer a strong contrast between the two scenarios, reflecting distinct driving demands and cognitive load associated with each scenario.

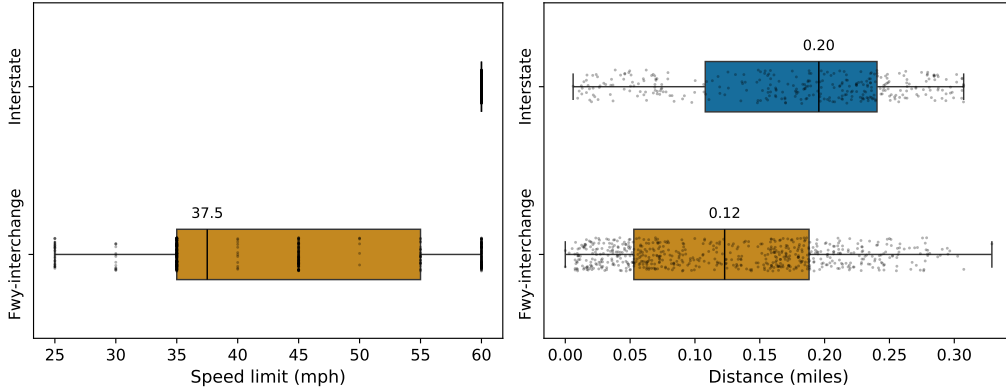


Figure 7: Boxplot distributions of the speed limit and trip distance for Interstate and Freeway-interchange roadways. The middle line shows the median speed limit and median route distances.

### 3.2. Executing Video-based Model

We conducted the section 2.4 experiments across the two representative scenarios with both transitional and straight driving maneuvers. The aim was to investigate whether the large vision model could capture the subtle visual features to effectively distinguish driving behavior relevant for cognitive assessment. The experiments were conducted under the following sampling protocols (step 4 in section 2.4):

- **Random Sampling:** Video segments are randomly split into train and test sets without enforcing driver-level separation.
- **Driver-level Separation (DLS):** A leave- $k$ -drivers-out cross-validation strategy is employed, where  $k = 5$  drivers were excluded during training and used exclusively for testing. This protocol was repeated over  $r = 3$  independent runs with different left-out driver groups and the final metrics were determined by averaging those runs.

In our experiments, the parameters were set as: (1) Input image size (960x752x3), (2) Vision model backbone: ResNet-v2 [41] (3) Video-to-vector dimension (6144x1), (4) Frame rate  $\{1, 10\}$  Hz, (5) Low-dimension size,  $n \in \{50, 100, 200\}$ , and (6) Distance metric: Euclidean distance. This setting provided a comprehensive understanding of how video-derived feature spaces behave under varying sampling conditions and data splits and laid the foundation for downstream classification tasks.

## 4. Results

### 4.1. Model Performance on Different Scenarios

Table 3: Model performance on two roadway types

Scenario categories	Accuracy (a)	Precision (P)	Recall (R)	F1 score (F1)	Sampling method
Fwy-int.	71.03%	0.7597	0.7728	0.7662	random
Interstate	55.12%	0.5404	0.5333	0.5368	random
$\Delta$	15.91%	0.1293	0.1395	0.1344	random
Fwy-int.	<b>69.81 <math>\pm</math> 2.51%</b>	0.7378 $\pm$ 0.0371	0.7624 $\pm$ 0.0671	0.7505	DLS
Interstate	52.17 $\pm$ 1.93%	0.5920 $\pm$ 0.0636	0.5997 $\pm$ 0.0771	0.5958	DLS
$\Delta_{ds}$	<b>17.64% <math>\uparrow</math></b>	0.1458 $\uparrow$	0.1627 $\uparrow$	0.1547 $\uparrow$	DLS

$\Delta$ : difference w/o DLS,  $\Delta_{ds}$ : difference w/ DLS, Fwy-int.: Freeway interchange, DLS: Driver-level Separation

As discussed in section 2.4, we trained two RF models to identify the aging-groups (Normal-aging vs. MD-aging) across the Freeway interchange and Interstate scenarios. Table 3 reveals the performance of the trained RF models. The  $\Delta$  row (without driver-level separation) indicates significant separation on all metrics (**a, P, R, F1**) and validates the selection of these contrastive scenarios to classify aging groups. The performance difference (grey rows) between the two scenarios indicates that there are prominent vision features in these specific scenarios that can successfully distinguish the aging groups solely by looking at the driving behavior features.

Furthermore, the driver-level separation yields slightly widened separation, which can be observed on all metrics (**a, P, R, F1**) in the  $\Delta_{ds}$  row. It surpassed the performance difference achieved without driver-level separation; for example, the accuracy difference went up from  $\Delta = 15.91\%$  to  $\Delta_{ds} = 17.64\%$ , indicating a 1.73% increment in performance difference. The  $\Delta_{ds}$  aligns with achieving a significant performance difference while there is no “subject-level overlapping”. It also validates that the Fwy-int scenario includes more prominent driving movement features compared to its counterpart. On the other hand, the Interstate scenario performs significantly worse, yielding lower accuracy and F1-score. Therefore, the Freeway interchange is a more behaviorally informative and cognitively sensitive driving scenario,

where complex maneuvers, short distances and lower speed variability have more nuanced driver responses.

We compared our results with a recent study [42] that used a multi-modal (demographics and sleep log data) framework to detect cognitive decline in older drivers. Our method outperformed both without Driver-level Separation ([42] accuracy 68.64% vs. our Fwy-int. accuracy 71.03%) and with Driver-level Separation ([42] accuracy 70.48% vs. our Fwy-int. max accuracy 72.32%) cases on the RWRAD dataset. This highlights the effectiveness of scenario-specific vision features as non-invasive digital biomarkers for cognitive aging classification. Moreover, another recent study by Danda et al. [43] found that amyloid-positive older adults exhibited higher average speeds, intermittent speed variability and increased acceleration on freeway on-ramp driving (similar to Fwy-int scenario), suggesting less adaptive driving. In clinical research, Amyloid is a protein that accumulates abnormally in the brain and forms plaques linked to the development of MD. Patients with cognitive impairment who test amyloid-positive are typically diagnosed as having MD, whereas amyloid-negative patients are generally excluded from an MD diagnosis [44, 45]. These findings confirm that Freeway ramp driving requires increased cognitive load involving behavioral reactions to rapidly changing traffic and abrupt speed shifts, combining perception with motor control [43]. Additionally, they underscore our results of higher classification accuracy ( $\mathbf{a} = 71.03\%$ ) and F1-score ( $\mathbf{F1} = 0.6712$ ) in Freeway interchange scenarios compared to the Interstate settings ( $\mathbf{a} = 55.12\%$ ,  $\mathbf{F1} = 0.5368$ ). Although their approach combined driving patterns with physiological signals, it validates the relevance of using contrastive and challenging roadway scenarios in cognitive assessment tasks. Therefore, this study supports our findings that the Freeway interchange scenario provides more informative and strong behavioral cues that the large vision model can leverage to better separate cognitive aging groups.

#### 4.2. Percentage of Misclassification

In this section, we assessed the feasibility of our Vision model-based approach by calculating the percentage of misclassification for all  $N = 69$  subjects (including normal and MD). For each subject  $k$ , we denote  $n_{\text{test}}^{(k)}$  represent the number of times they appeared in the test set across 10 resamples, and  $n_{\text{error}}^{(k)}$  denote the number of times they were misclassified by the RF

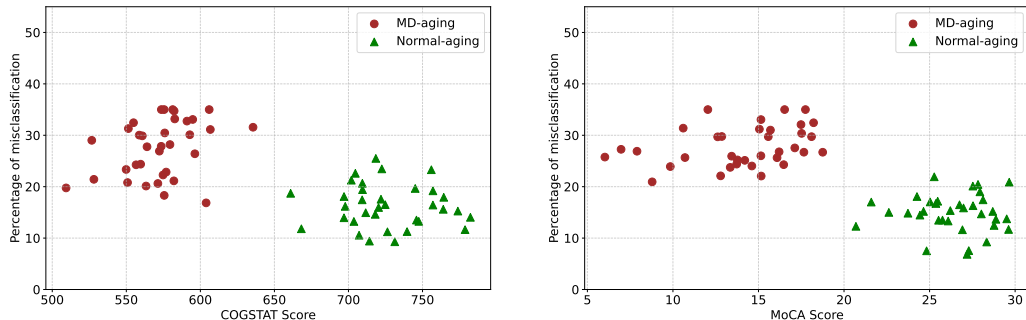


Figure 8: Percentage of misclassification vs. - (a) COGSTAT score and (b) MoCA score. The relevant route segments were filtered out from the Omaha most transited route database shown in Figure 3.

classifier. The subject-specific misclassification rate is then calculated as:

$$\% \text{ of missclassification}^{(k)} = 100 \times \left( \frac{n_{\text{error}}^{(k)}}{n_{\text{test}}^{(k)}} \right)$$

Figure 8 displays the relationship between misclassification percentage and cognitive scores. An overall trend observed was that subjects labeled as MD-aging tend to exhibit higher misclassification percentages compared to the Normal-aging drivers. This is evident in the middle cognitive score ranges (COGSTAT: 580–650; MoCA: 12–20), where the misclassification is higher. It suggests that the middle zones correspond to a transition region where the classifier shows more uncertainty, due to the overlapping feature space between early-stage impairment and Normal-aging. In addition, it underscores the anticipated challenge of reliably distinguishing subtle cognitive impairments from Normal-aging. On the other hand, subjects with low (COGSTAT < 550 and MoCA < 8) and high (COGSTAT > 700 and MoCA > 20) cognitive scores consistently yield lower misclassification rates. This behavior indicates that the classifier learned prominent feature representations in these regions and it is able to classify the aging groups more confidently. Additionally, it reinforces the validity of using COGSTAT and MoCA as effective biomarkers in well-separated diagnostic states. Overall, these trends are consistent with the model’s performance as reported in Table 3. The global performance and localized misclassification patterns support the interpretation that the model’s predictive success is not random but

rather driven by the prominent vision signals yielded from a certain cognitive state. Subjects with well-defined cognitive profiles were more reliably classified. However, uncertainty increased in transitional cognitive states, reflecting appropriate model sensitivity to the early-stage classification. This behavior supports the validity of our approach and suggests that further improvement may require incorporating auxiliary clinical signals to resolve the transition zone uncertainty. Overall, this subject-level metric captures individual classification stability and uncertainty at the subject level.

#### *4.3. Limitations and Future Works*

The current dataset is constrained to a limited number of driving scenarios, which might not cover the full range of real-world driving complexity (e.g., night driving, inclement weather, heavy traffic). Future work can include a broader set of driving scenarios to generalize findings across real-world traffic and environmental conditions. The driver-level separation was limited to a 3-fold cross-validation with a small pool of test subjects. This can lead to variance in performance estimation and may not generalize well to other populations and road infrastructures. Recruiting more diverse drivers and conducting longitudinal assessments would strengthen generalization. Additionally, the number of dementia subjects in the study was relatively small ( $N = 9$ ). Including more dementia participants would guarantee the statistical validity of the findings and provide deeper insights into the driving cues associated with dementia. Moreover, the use of in-vehicle video recording raises potential concerns regarding privacy. Future implementations should address these with robust data management. Another notable limitation is the relatively limited availability of high-quality in-vehicle video data per cognitive group. The model’s misclassification rates, particularly in the transitional region, were influenced by this data scarcity. We believe that scaling up the dataset with higher-quality video samples for both cognitively normal and dementia groups will allow the method to extract more meaningful and generalizable features. This would be especially critical for improving video analysis accuracy in cases with confusing behavioral features.

## **5. Conclusion**

This study highlights the potential of monitoring real-world driving behavior as a valuable tool for early cognitive health assessment in older adults. The results suggest that scenario-based analysis plays a significant role in

video-based cognitive assessment. By segmenting driving video data into semantically distinct scenarios, our approach enables targeted driving behavior analysis under specific cognitive demands. In the scope of this work, freeway interchange scenarios yield significantly higher classification performance compared to interstate scenarios under driver-level separation. Therefore, certain driving scenes inherently capture richer behavioral variance, which large vision models can leverage to distinguish between cognitive aging driving patterns. This approach offers a low-cost, scalable alternative to traditional cognitive screening methods, enabling passive and non-intrusive cognitive monitoring. It has direct implications for the healthcare industry, where early detection of cognitive decline remains a costly and time-consuming process. Additionally, the ability to extract digital biomarkers from routine driving behavior transforms personal vehicles into affordable diagnostic tools. This reduces patient burden while supporting continuous and longitudinal health assessment. Moreover, it holds promise in providing an efficient screening tool for aging populations in early detection of cognitive decline, especially in areas with limited access to healthcare facilities.

## **6. Acknowledgements**

This work was supported by the National Institutes of Health (NIH), the National Institute on Aging (NIA 5R01AG17177-18), and the University of Nebraska Medical Center Mind & Brain Health Labs. The views expressed in this paper are those of the authors alone and not the NIH or NIA. We thank our research team for coordinating this project. Due to personally identifying information (PII), the data are not available online. The authors declare no potential conflict of interest.

## **Appendix A. Study Recruitment Criteria**

The inclusion and exclusion criteria used for participant recruitment are summarized in Table A.4.

## **Appendix B. Cognitive Tests used for COGSTAT score**

Cognitive Tests used for calculating COGSTAT score in the RWRAD dataset across five cognitive domains [9] are summarized in Table B.5.

Table A.4: Participant inclusion and exclusion criteria [32]

Inclusion Criteria	Exclusion Criteria
(a) age between 65 and 90 years	(a) pulmonary disease requiring chronic medication
(b) residing independently in Nebraska or nearby states (e.g., Iowa)	(b) Congestive heart failure
(c) possession of a valid driver’s license	(c) major psychiatric illness
(d) met Nebraska visual acuity standards (> 20/50 OU, corrected or uncorrected)	(d) active vestibular disease
(e) proficiency in English	(e) substance abuse within one year prior to enrollment
(f) capability to provide informed consent	(f) use of medications that could confound study outcome
	(g) clinical or neurological conditions (e.g., stroke) that could interfere with the study outcome

## References

- [1] J. J. Manly, R. N. Jones, K. M. Langa, L. H. Ryan, D. A. Levine, R. McCammon, S. G. Heeringa, D. Weir, Estimating the prevalence of dementia and mild cognitive impairment in the us: The 2016 health and retirement study harmonized cognitive assessment protocol project, *JAMA Neurology* 79 (12) (2022) 1242–1249.
- [2] R. Roberts, D. S. Knopman, Classification and epidemiology of mci, *Clinics in geriatric medicine* 29 (4) (2013) 10–1016.
- [3] N. D. Anderson, State of the science on mild cognitive impairment (mci), *CNS spectrums* 24 (1) (2019) 78–87.
- [4] P. Chen, H. Cai, W. Bai, Z. Su, Y.-L. Tang, G. S. Ungvari, C. H. Ng, Q. Zhang, Y.-T. Xiang, Global prevalence of mild cognitive impairment among older adults living in nursing homes: a meta-analysis and systematic review of epidemiological surveys, *Translational Psychiatry* 13 (1) (2023) 88.
- [5] C. Laske, H. R. Sohrabi, S. M. Frost, K. L. de Ipiña, P. Garrard, M. Buscema, J. Dauwels, S. R. Soekadar, S. Mueller, C. Linnemann,

Table B.5: Cognitive Tests conducted for the COGSTAT composite score.

<b>Cognitive Domain</b>	<b>Cognitive Test</b>
(1) Memory	Benson, Recall Craft Story Delay, Verbatim HVLТ, Delay
(2) Language	Category Fluency, Animals Category Fluency, Vegetables MINT
(3) Visuospatial	Benson, Copy WAIS Blocks
(4) Executive Function	Trails B Verbal Fluency (F) Verbal Fluency (L)
(5) Attention	Trails A Number Span Forward (Total correct) Number Span Backward (Total correct)

Note: If all cognitive tests are the same as the mean, final COGSTAT will be  $14 \times 50 = 700$

S. A. Bridenbaugh, Y. Kanagasingham, R. N. Martins, S. E. O’Bryant, Innovative diagnostic tools for early detection of alzheimer’s disease, *Alzheimer’s & Dementia* 11 (5) (2015) 561–578.

- [6] C. L. Allan, S. Behrman, K. P. Ebmeier, V. Valkanova, Diagnosing early cognitive decline—when, how and for whom?, *Maturitas* 96 (2017) 103–108.
- [7] S. Bayat, G. M. Babulal, S. E. Schindler, A. M. Fagan, J. C. Morris, A. Mihailidis, C. M. Roe, Gps driving: a digital biomarker for preclinical alzheimer disease, *Alzheimer’s Research & Therapy* 13 (1) (2021) 115.
- [8] M. Rizzo, Impaired driving from medical conditions: a 70-year-old man trying to decide if he should continue driving, *Jama* 305 (10) (2011) 1018–1026.
- [9] C. R. Jack Jr, D. A. Bennett, K. Blennow, M. C. Carrillo, B. Dunn, S. B.

- Haeberlein, D. M. Holtzman, W. Jagust, F. Jessen, J. Karlawish, et al., NIA-AA research framework: toward a biological definition of Alzheimer's disease, *Alzheimer's & dementia* 14 (4) (2018) 535–562.
- [10] L. Chouliaras, J. T. O'Brien, The use of neuroimaging techniques in the early and differential diagnosis of dementia, *Molecular Psychiatry* 28 (10) (2023) 4084–4097.
- [11] T. Jitsuishi, A. Yamaguchi, Searching for optimal machine learning model to classify mild cognitive impairment (mci) subtypes using multimodal MRI data, *Scientific Reports* 12 (1) (2022) 4284.
- [12] V. S. Rallabandi, K. Seetharaman, Deep learning-based classification of healthy aging controls, mild cognitive impairment and Alzheimer's disease using fusion of MRI-PET imaging, *Biomedical Signal Processing and Control* 80 (2023) 104312.
- [13] R. Ossenkoppele, A. Pichet Binette, C. Groot, R. Smith, O. Strandberg, S. Palmqvist, E. Stomrud, P. Tideman, T. Ohlsson, J. Jögi, et al., Amyloid and tau PET-positive cognitively unimpaired individuals are at high risk for future cognitive decline, *Nature medicine* 28 (11) (2022) 2381–2387.
- [14] J. A. Pradeepkiran, J. Baig, M. A. Islam, S. Kshirsagar, P. H. Reddy, Amyloid- $\beta$  and phosphorylated tau are the key biomarkers and predictors of Alzheimer's disease, *Aging and disease* 16 (2) (2024) 658.
- [15] G. Grande, M. Valletta, D. Rizzuto, X. Xia, C. Qiu, N. Orsini, M. Dale, S. Andersson, C. Fredolini, B. Winblad, et al., Blood-based biomarkers of Alzheimer's disease and incident dementia in the community, *Nature Medicine* (2025) 1–9.
- [16] J. Zhang, Y. Zhang, J. Wang, Y. Xia, J. Zhang, L. Chen, Recent advances in Alzheimer's disease: Mechanisms, clinical trials and new drug development strategies, *Signal transduction and targeted therapy* 9 (1) (2024) 211.
- [17] Y. G. Rykov, M. D. Patterson, B. A. Gangwar, S. B. Jabar, J. Leonardo, K. P. Ng, N. Kandiah, Predicting cognitive scores from wearable-based digital physiological features using machine learning: data from a clinical trial in mild cognitive impairment, *BMC medicine* 22 (1) (2024) 36.

- [18] R. Whelan, F. M. Barbey, M. R. Cominetti, C. M. Gillan, A. M. Rosická, Developments in scalable strategies for detecting early markers of cognitive decline, *Translational Psychiatry* 12 (1) (2022) 473.
- [19] C. Xue, S. S. Kowshik, D. Lteif, S. Puducheri, V. H. Jasodanand, O. T. Zhou, A. S. Walia, O. B. Guney, J. D. Zhang, S. Poésy, et al., Ai-based differential diagnosis of dementia etiologies on multimodal data, *Nature Medicine* 30 (10) (2024) 2977–2989.
- [20] E. Khodabandehloo, D. Riboni, A. Alimohammadi, Healthxai: Collaborative and explainable ai for supporting early diagnosis of cognitive decline, *Future Generation Computer Systems* 116 (2021) 168–189.
- [21] Q. Lin, C. Che, H. Hu, X. Zhao, S. Li, A comprehensive study on early alzheimer’s disease detection through advanced machine learning techniques on mri data, *Academic Journal of Science and Technology* 8 (1) (2023) 281–285.
- [22] J. B. Langbaum, J. Zissimopoulos, R. Au, N. Bose, C. J. Edgar, E. Ehrenberg, H. Fillit, C. V. Hill, L. Hughes, M. Irizarry, et al., Recommendations to address key recruitment challenges of alzheimer’s disease clinical trials, *Alzheimer’s & Dementia* 19 (2) (2023) 696–707.
- [23] L. P. Kostyniuk, L. J. Molnar, Self-regulatory driving practices among older adults: Health, age and sex effects, *Accident Analysis & Prevention* 40 (4) (2008) 1576–1580.
- [24] J. D. Davis, G. D. Papandonatos, L. A. Miller, S. D. Hewitt, E. K. Festa, W. C. Heindel, B. R. Ott, Road test and naturalistic driving performance in healthy and cognitively impaired older adults: does environment matter?, *Journal of the American Geriatrics Society* 60 (11) (2012) 2056–2062.
- [25] D. W. Eby, N. M. Silverstein, L. J. Molnar, D. LeBlanc, G. Adler, Driving behaviors in early stage dementia: A study using in-vehicle technology, *Accident Analysis & Prevention* 49 (2012) 330–337.
- [26] X. Di, R. Shi, C. DiGuseppi, D. W. Eby, L. L. Hill, T. J. Mielenz, L. J. Molnar, D. Strogatz, H. F. Andrews, T. E. Goldberg, et al., Using naturalistic driving data to predict mild cognitive impairment and

- dementia: preliminary findings from the longitudinal research on aging drivers (longroad) study, *Geriatrics* 6 (2) (2021) 45.
- [27] B. R. Ott, R. N. Jones, R. B. Noto, D. C. Yoo, P. J. Snyder, J. N. Bernier, D. B. Carr, C. M. Roe, Brain amyloid in preclinical alzheimer's disease is associated with increased driving risk, *Alzheimer's & Dementia: Diagnosis, Assessment & Disease Monitoring* 6 (2017) 136–142.
- [28] N. V. Dokholyan, R. C. Mohs, R. J. Bateman, Challenges and progress in research, diagnostics, and therapeutics in alzheimer's disease and related dementias, *Alzheimer's & Dementia: Translational Research & Clinical Interventions* 8 (1) (2022) e12330.
- [29] J. Merickel, R. High, J. Dawson, M. Rizzo, Real-world risk exposure in older drivers with cognitive and visual dysfunction, *Traffic injury prevention* 20 (sup2) (2019) S110–S115.
- [30] R. O. Hettiarachchige, M. J. Rapoport, G. Naglie, E. Vingilis, J. Seeley, S. Alizadeh, S. Bayat, Common driving behaviors in older adults with dementia: Insights from a systematic literature review, *Alzheimer's & Dementia* 21 (6) (2025) e70340.
- [31] J. M. Doherty, S. A. Murphy, S. Bayat, J. K. Wisch, A. M. Johnson, A. Walker, S. E. Schindler, B. M. Ances, J. C. Morris, G. M. Babulal, Adverse driving behaviors increase over time as a function of preclinical alzheimer's disease biomarkers, *Alzheimer's & Dementia* 19 (5) (2023) 2014–2023.
- [32] J. H. Chang, Y. Huang, Y. Zhang, S. Chen, D. L. Murman, V. Phatak, M. Rizzo, Day-to-day sleep efficiency and driving behaviors in older adults with and without cognitive impairment, *medRxiv* (2025) 2025–02.
- [33] M. S. Albert, S. T. DeKosky, D. Dickson, B. Dubois, H. H. Feldman, N. C. Fox, A. Gamst, D. M. Holtzman, W. J. Jagust, R. C. Petersen, et al., The diagnosis of mild cognitive impairment due to alzheimer's disease: recommendations from the national institute on aging-alzheimer's association workgroups on diagnostic guidelines for alzheimer's disease, *Alzheimer's & dementia* 7 (3) (2011) 270–279.

- [34] M. Rizzo, J. Sparks, S. McEvoy, S. Viamonte, I. Kellison, S. P. Vecera, Change blindness, aging, and cognition, *Journal of Clinical and Experimental Neuropsychology* 31 (2) (2009) 245–256.
- [35] Z. S. Nasreddine, N. A. Phillips, V. Bédirian, S. Charbonneau, V. Whitehead, I. Collin, J. L. Cummings, H. Chertkow, The montreal cognitive assessment, moca: a brief screening tool for mild cognitive impairment, *Journal of the American Geriatrics Society* 53 (4) (2005) 695–699.
- [36] L. Rizzi, I. Rosset, M. Roriz-Cruz, Global epidemiology of dementia: Alzheimer’s and vascular types, *BioMed Research International* 2014 (1) (2014) 908915.
- [37] A. Kolesnikov, L. Beyer, X. Zhai, J. Puigcerver, J. Yung, S. Gelly, N. Houlsby, Big transfer (bit): General visual representation learning, in: *Computer Vision—ECCV 2020: 16th European Conference, Glasgow, UK, August 23–28, 2020, Proceedings, Part V* 16, Springer, 2020, pp. 491–507.
- [38] S. Wold, K. Esbensen, P. Geladi, Principal component analysis, *Chemometrics and Intelligent Laboratory Systems* 2 (1) (1987) 37–52, proceedings of the Multivariate Statistical Workshop for Geologists and Geochemists.
- [39] L. Breiman, Random forests, *Machine learning* 45 (2001) 5–32.
- [40] G. Cawley, Leave-one-out cross-validation based model selection criteria for weighted ls-svms, in: *The 2006 IEEE International Joint Conference on Neural Network Proceedings, 2006*, pp. 1661–1668.
- [41] K. He, X. Zhang, S. Ren, J. Sun, Identity mappings in deep residual networks, in: *European conference on computer vision*, Springer, 2016, pp. 630–645.
- [42] A. Joshi, J. H. Chang, G. Basulto-Elias, S. Hallmark, M. Rizzo, A. Sharma, Identifying and predicting cognitive decline using multi-modal sensor data and machine learning approach, *Research Square* (2025) rs-3.
- [43] S. S. R. Danda, Y. L. Murphy, A. C. Maher, C. C. Persad, J. R. Bross, E. Flynn, R. A. Koeppe, B. Giordani, Detection of differences between

amyloid-positive and negative participants based on their driving behavior during on-ramp merging, *Alzheimer's & Dementia* 20 (S3) (2024) e089345.

- [44] B. Souchet, A. Michail, B. Billoir, J. Braudeau, Biological diagnosis of alzheimer's disease based on amyloid status: An illustration of confirmation bias in medical research?, *International Journal of Molecular Sciences* 24 (24) (2023) 17544.
- [45] M. Bilgel, S. M. Resnick, Amyloid positivity as a risk factor for memory decline and lower memory performance as an indicator of conversion to amyloid positivity: Chicken and egg, *Biological Psychiatry* 87 (9) (2020) 782–784.